

Using Minimum Actuators to Control Shape and Stress of a Double Layer Spherical Model Under Gravity and Lateral Loadings

Najmadeen Saeed^{1,2}, Javad Katebi³, Ahmed Manguri^{1,4*}, Aram Mahmood³,
Marcin Szczepanski⁴, Robert Jankowski⁴

¹ Civil Engineering Department, University of Raparin, Rania, Kurdistan Region, Iraq

² Civil Engineering Department, Tishk International University, Erbil, Kurdistan Region, Iraq

³ Faculty of Civil Engineering University of Tabriz, Tabriz, Iran

⁴ Faculty of Civil and Environmental Engineering, Gdansk University of Technology, Gdansk, Poland

* Corresponding author's e-mail: ahmed.manguri@pg.edu.pl

ABSTRACT

Spherical domes are picturesque structures built in developed countries to attract tourists. Due to horizontal and vertical overloading, the structures' attractive shapes may be disturbed, and some members' stress may exceed the elastic level. In this paper, the shape and stress of a deformed double-layer spherical numerical model due to simultaneous lateral and vertical loadings are controlled, meanwhile, the number of actuators to alter the length of active members is minimized. The nodal displacements of the outer shape of the numerical model of the double-layer spherical structure are nullified. In addition, the stress of the members of the structure was monitored to stay within the elastic level. Moreover, the number of used actuators was minimized. These objectives are done by subjecting controlling formulations to a function that finds the minimum of constrained nonlinear multivariable which is called *fmincon*. The defined function in MATLAB uses one of the optimization algorithms (sequential quadratic programming, interior point, trust-region reflective, and active set). The algorithms search for active members that have a significant influence in controlling the targeted joints and members. Furthermore, the algorithms exclude the inactive actuators in several loops. The results obtained from MATLAB program are validated by SAP2000 software.

Keywords: spherical structures, double layer structures, actuators, shape and stress control, optimization, *fmincon* function.

INTRODUCTION

Reshaping the misshapen architectural structures due to loadings is greatly appreciated by architects. In the modern world, constructing attractive symbolic architectural structures is challenging. Spherical structures are considered a picturesque construction that can be found in several places around the world, such as the Pavilion and Science Museum (Nur Alem) in Kazakhstan [1, 2] and the Ericsson Globe in Stockholm, Sweden [3]. Due to their large free column space and different loading cases, such as vertical and lateral ones, the appearance of such structures is susceptible to distortion. For this reason,

researchers have been giving solutions to control the structural geometry after loading via changing the length of some members. Irschik [4] stated that the change in a node's position, which significantly affects the appearance of structures, can be done by changing the length of some active members. In addition, Haftka [5] reported that the change in the members' length can be done via an actuator tool.

Different types of actuators are implemented for shape and stress condoling of structures, for example, piezoceramic actuators are utilized to obtain the required shape of flexible structures [6] and composite structures [7, 8]. Moreover, Haftka and Adelman [9] applied temperature to alter the

length of some members of space structures. Furthermore, other types of actuators were embedded in members of structures, for example, lead active screw members [10] and mechanical actuators [11].

The idea of shape controlling was introduced by Weeks [12] and then analytically presented by Haftka and Adelman [13], while its computational aspects were described by Ziegler [14]. The shape of structures is defined by their nodal coordinates; therefore, the joint displacements of sensitive structures and those that undergo significant deformations are required to be reshaped. Space structures require high surface accuracy, such as antennas that transfer signals [15, 16]. In addition, the shape of architectural structures is essential [17]; thus, reforming the disturbed geometry is indispensable.

Researchers applied the techniques of shape adjustment to several structures, for example cable mesh structures [18, 19] and cable-stayed bridges [20]. In addition, Du, Zong [21] implemented SQP algorithm to control the shape of a cable mesh antenna. The action of shape controlling which is done via changing the length of some members, may cause inducing excessive stress in some members that may end up in member failure. For this reason, in line with nodal displacement control, the stress of the members should be monitored, especially for the large span structures stress is one of the main causes of failure [22].

Although the shape distortion of structures is controllable, the stress in some members exceeds the limit due to changing their lengths. Saeed and Kwan [11] introduced a technique based on the Force Method to simultaneously control displacement and internal force. Moreover, axial force control of prestressable trusses has been detailed by Kwan and Pellegrino [23]. The approach of shape and stress control has been applied to different structures, for instance, trusses [24, 25], cable structures [26, 27], and cable arch-stayed bridges [20]. Besides controlling the shape and stress of structures, researchers tried to optimize the cost of undertaking it.

Structural optimization opened a new chapter in structural engineering [28] and mechanical engineering [29]. Researchers found out that the location of the actuators is significant in controlling the shape and stress of members [23, 30]. Reducing the actuator numbers has been done for cable net structures [31, 32], and space structures under lateral [33] and vertical loadings [34, 35]. At the same time, studies have not been conducted

regarding shape and stress controlling of spherical structures, under the effect of vertical and horizontal loadings simultaneously.

In this research, a deformed numerical model of a double-layer spherical structure is reshaped; meanwhile, the internal force of all members is assumed to be within the elastic range. Furthermore, the number of implemented actuators is minimized, and the amount of actuation is also optimized by using optimization algorithms (sequential quadratic programming (SQP), interior point, trust-region reflective, and active set) [36].

METHODOLOGY

Numerical geometry of the spherical structure and loading

The numerical model of the pin-jointed structure is designed to have an overall diameter of 8m, it is formed by two connected layers; their center-to-center distance is set to be 200mm. The ratio of the thickness of the layers to the height of the structure should be within the range of 1/30 to 1/60 [37]. Furthermore, the internal layer contains 200 joints and 420 members, while the external one is formed by 182 Joints and 380 members, the two layers connected by 720 members. The length of the members varies from 185.99mm to 1251.5mm; their length depends on the coordination of the two connected joints. It should be highlighted that the connections are pin-jointed, and the 20 bottom joints were restrained against the three-dimensional translation, as shown in Figure 1.

To make the numerical model close to practice as much as possible, and taking the most critical condition of loading, which is simultaneously loading the structure in two directions that cause extensive shape deformation and inequality stress distribution in members. For this purpose, the 101 free exterior joints were loaded with 9000N gravity loading (Z-direction) and 73 joints were loaded with 1145N lateral loadings (X-direction) as presented in Figure 1.

Material properties

The geometry and the material's physical properties were selected so that the structure gets challenging deformation and stress distribution after applying the external loadings. Furthermore, the members have 15 mm diameter, 200

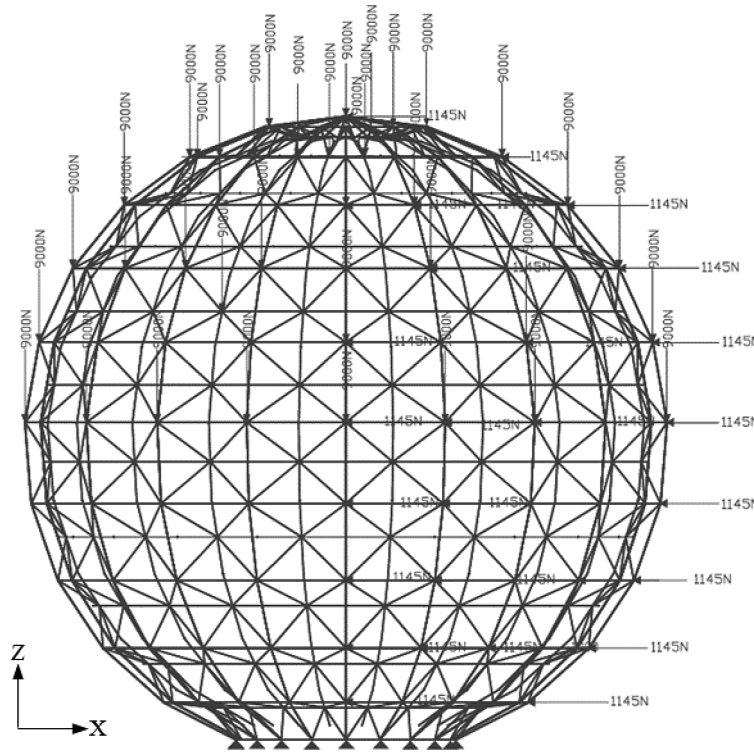


Figure 1. Vertical and lateral loads of the numerical model

GPa elasticity modulus, and 420MPa yield stress. It should be mentioned that the self-weight of the members has been neglected.

The maximum allowable axial force can be found as follows:

$$t_{all} = \sigma_y * A = 420 * \pi * 7.5^2 = 74220N$$

where: t_{all} – the allowable axial force (tension or compression) in the members.

Analysis, adjustment, and optimization

To construct the numerical model in MATLAB, intensive code has been developed to generate the nodal coordinates and to connect the joints by bars. The coordinates and bar connectivity found in MATLAB are input into SAP2000 software to verify the analysis of the structure before performing shape adjustment. After loading the structure, the induced joint displacements and internal forces can be obtained. A target is set regarding reducing or nullifying the nodal displacements and redistributing the members' stress; the data input in Equations 1 and 2 in MATLAB to obtain the optimum set of actuation to reshape and redistribute the stress in members; the detailed procedure has presented the flowchart in Figure 2.

$$\begin{aligned} Y e_o &= d_{tar} - d_p \\ Z e_o &\leq t_p - t_{tar} \end{aligned} \quad (1)$$

where: Y is the matrix arranged by rows and columns representing the targeted joints and the selected actuators respectively, e_o is the actuation set, d_{dar} and d_p are the prescribed and induced displacements due to loading. While, Z is the matrix is formed through the relation of the targeted members and the selected actuators, t_p and t_{dar} are the induced and targeted internal force due to applied loads.

Equation (2), the optimization function available in MATLAB under the fmincon function, is subjected to Equation (1). The function relies on optimization algorithms (SQP, interior point, trust-region reflective, and active set). The purpose of using Equation (2) is to find the least possible actuation with the fewest possible number of actuators to undertake shape and stress controlling in Equation (1). The function works so that the inactive members to undertake adjustment are identified and excluded to reduce the used actuators.

$$\min f(x) = \sum_{i=1}^n e_{oi} \quad (2)$$

Where n is the number of actuators. In each step, inactive members are excluded, the procedure is repeated until the actuators with $|e_o| \leq 0.1$ are ended (actuation less than 0.1mm is unpragmatic), and the error percentage is found for each step. The differences between the targets and the results should be negligible; otherwise, resection bars are done. If the discrepancy between the results and the goals were insignificant and there were no more $|e_o| \leq 0.1$ this will be the optimum set of e_o , (see Figure 2). After obtaining the optimal e_o , it can be applied to the structure in MATLAB and SAP2000 to verify the results.

RESULTS AND DISCUSSION

Due to the loadings, the structure underwent significant deformations, as shown in Figure 3,

the nodal displacements in the loading directions (X and Z) were noticeable, as presented in Table 1, and the movements in Y-direction were minor. Table 1 shows that the maximum displacement in Z and X directions were 31.5 and 44.6 mm, respectively. Since the spherical structures are architectural essentials and are considered attractive elements, their distorted form should be reshaped. In this work, attempts have been made to reshape the spherical structure’s outer face while the members’ stress was also estimated to be within the elastic limit. Furthermore, optimization techniques were implemented with the adjustment equations to minimize the actuator numbers and miniaturize the amount of actuation.

The goals were set to bring the outer layer joints to their origin (their coordinates before the loading) and keep all members’ stress within the elastic range. Furthermore, for simplicity and practicality, a limit was set for actuators (i.e., all actuators with less than 0.1mm should be excluded). In the beginning, it was assumed that all members were embedded with actuators, then the

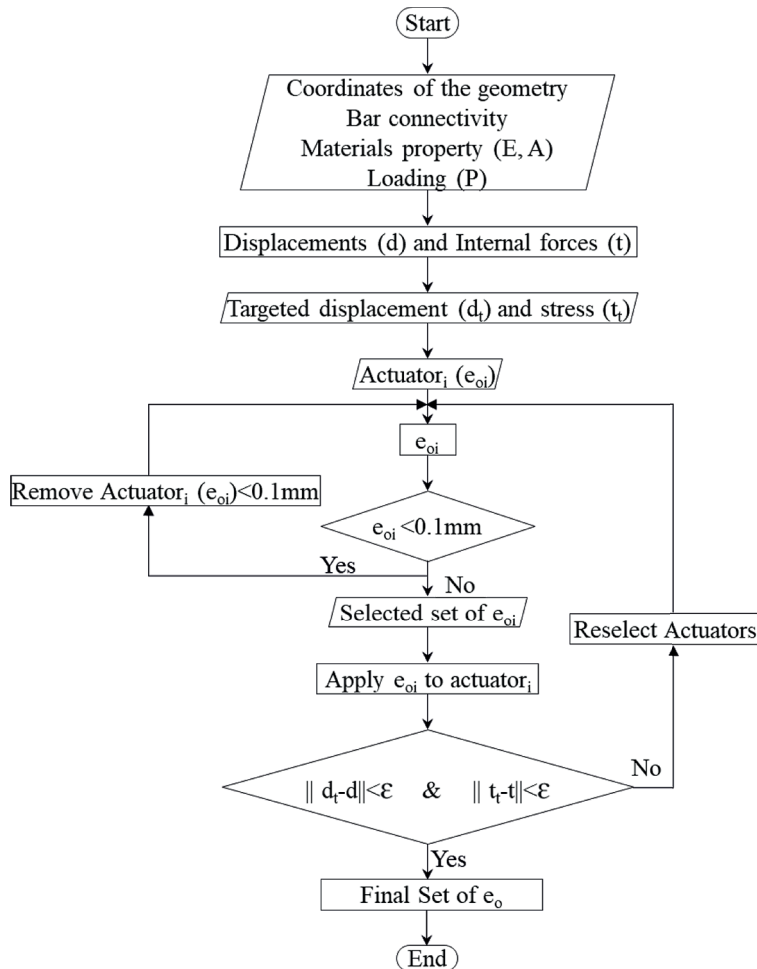


Figure 2. The strategy of the work

algorithm reduced the actuators by excluding inactive ones such that the actuators with less than the limit will be taken out for the next step. The algorithm took 22 steps to obtain the optimum set of actuation with the minimum possible number of actuators (see Figure 4) and minimum amount of actuation (see Figure 5), while the targets in terms of joint displacements and axial force in members were preserved.

Figure 4 illustrates the algorithm's effectiveness in miniaturizing the number of actuators in 22 steps. It can be seen that there was a dramatic fall in the number of actuators; in the first step, more than 250 inactive members were excluded. In step 15, almost half of the members were excluded from being embedded with actuators. Furthermore, there was a negligible increase in the slope negativity of the curve from steps 10 to 15, while there was a rapid fall of the line from steps 15 to 19 (see Figure 4); this also caused the fluctuation of the curve shown in Figure 5. Finally, in step 22, only 679 members remained involved as actuators; in other words, there were no more actuators with less than $|0.1|mm$, the amount of actuation per actuator presented in Table 2.

Figure 5 illustrates the total amount of actuation in 22 steps. However, in the 1st step, the amount of actuation was minimum, participating

all members as actuators is neither pragmatic nor economic. It should be highlighted that; the fundamental goal is to reshape the structure and keep it safe in terms of stress with the optimum number of actuators. This is because embedding actuators is more costly than performing actuation. It can be seen that from the figure, in steps where the number of the excluded actuators was large, there was an increase in the amount of actuation, this is due to the fact that the amount of the actuation taken by the excluded actuators was distributed on the remained ones. The total amount of actuation in step 22 was 672mm; in each step, the dissimilarity between the obtained results after adjustment should be compared with the targets to see the percentage of error, as shown in Figure 6.

Figure 6 illustrates a negligible discrepancy between the targets and the obtained results after adjustment. It means that the technique works well in terms of reaching goals. It can be said that the exterior joints' displacements were nullified, and the stress in all members was kept within the elastic range, as presented in Table 3.

Table 2 shows the members and their value of actuation, the maximum shortened and lengthened values were 12.5mm, and 18.45mm respectively. The majority of the members that were embedded with actuators were lengthened.

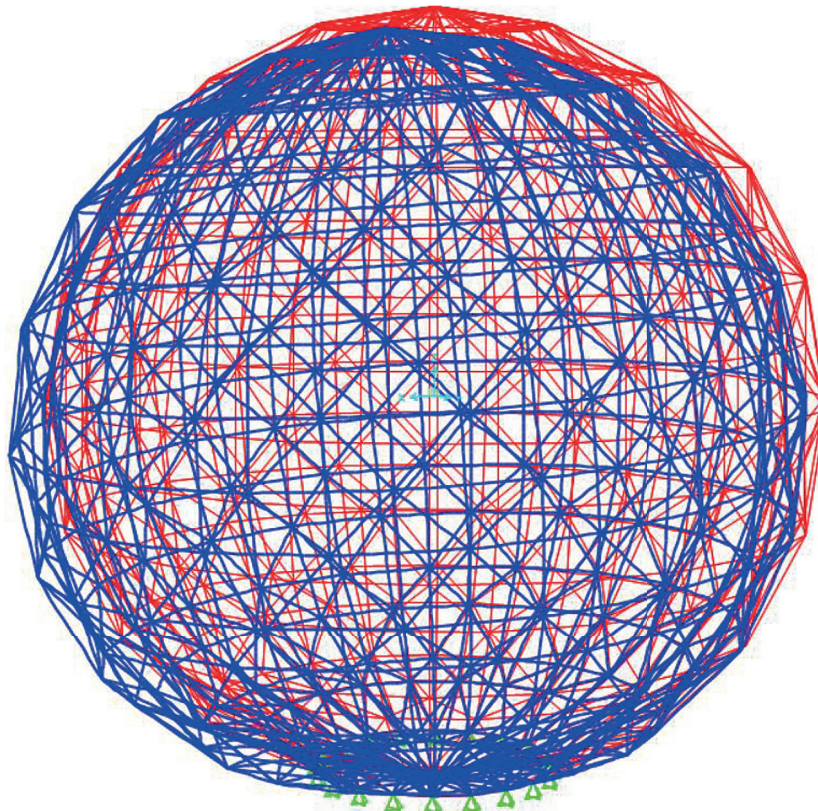


Figure 3. The original and deformed shape of the numerical model

Table 1. The joint displacements before the adjustment in z and x directions using MATLAB and SAP2000

z-dp (mm)	Joints	x-dp (mm)	Joints
-31.5to-30	81, 101, 82, 100, 300, 281, 120, 102	44.6to44	382, 167, 168, 166, 169, 165, 170, 164, 171
-29.9to-28	61, 261, 280, 320, 301, 121, 62, 80, 299, 282, 140, 122	43.9to42	368, 367, 369, 163, 366, 370, 365, 172, 371, 364, 162, 372, 363, 173, 373, 362, 161, 374, 174, 361, 180, 375, 380, 175, 376, 379, 377, 179, 378, 176, 178, 177, 347, 346, 348, 345, 344, 349, 146, 147, 145, 343, 350
-27.9to-26	262, 279, 319, 302, 83, 99, 119, 103, 241, 260, 340, 321	41.9to40	148, 144, 342, 149, 351, 143, 341, 150, 352, 142, 360, 353, 151, 359, 354, 141, 358, 355, 152, 357, 356, 160
-25.9to-24	63, 41, 139, 79, 123, 141, 339, 322, 242, 259, 42, 60, 160, 142, 298, 283, 318, 303, 263, 278	39.9to38	153, 159, 325, 154, 324, 326, 158, 323, 155, 157, 327, 156, 322, 328, 321, 329, 125, 124
-23.9to-22	159, 143, 341, 360, 118, 104, 84, 338, 98, 323, 43, 59, 342, 359, 138, 124, 243, 258	37.9to36	126, 340, 123, 330, 127, 122, 339, 128, 331, 338, 121, 129, 332, 337, 333, 336, 334, 130, 140
-21.9to-20	64, 78, 221, 240, 161, 343, 358, 162, 180, 144, 158, 222	35.9to34	335, 139, 131, 304, 303, 305, 302, 138, 132, 306, 301, 137, 133
-19.9to-18	239, 297, 284, 317, 304, 163, 179, 337, 324, 264, 277, 44, 58, 344, 357, 164, 178	33.9to32	307, 134, 136, 135, 320, 308, 104, 103, 319, 105, 309, 106, 102
-17.9to-16	244, 257, 223, 238, 117, 105, 380, 137, 361, 125, 145, 157, 379, 362, 85, 97, 21, 378, 165, 22, 177, 363, 40, 65, 77	31.9to30	318, 310, 107, 101, 317, 311, 108, 120, 316, 312, 109, 315, 313, 314
-15.9to-14	345, 356, 377, 364, 336, 325, 23, 39, 376, 365, 316, 305, 166, 176, 45, 57, 224, 237, 296, 285, 366, 375	29.9to28	119, 283, 284, 282, 110, 285, 281, 118, 111, 286, 117, 300
-13.9to-12	382, 146, 156, 265, 276, 367, 355, 346, 374, 24, 38 175 167, 245, 256, 368, 373, 126, 136	27.9to26	112, 287, 116, 113, 299, 115, 114, 288, 83, 84, 82, 85, 298, 289
-11.9to-10	369, 372, 370, 371, 106, 116, 174, 168, 326, 335, 86, 96, 225, 236, 354, 347, 25, 37	25.9to24	86, 81, 297, 290, 87, 100, 296, 291, 88
-9.9to-8	66, 76, 155, 147, 173, 169, 46, 56, 306, 315, 172, 170, 171, 353, 348, 286, 295	23.9to22	295, 292, 99, 262, 263, 294, 293, 264, 261, 89, 265, 98, 280, 90
-7.9to-6	275, 266, 26, 36, 127, 135, 255, 246, 327, 334, 352, 349, 235, 226, 154, 148	21.9to20	266, 97, 279, 91, 267, 96, 92, 63, 62,,278, 95, 64, 93, 268, 94
-5.9to-4	351, 350, 107, 115, 55, 47, 95, 87, 201, 220, 35, 27	19.9to18	61, 65, 269, 277, 80, 66, 270, 242, 276, 241
-3.9to-2	307, 314, 202, 75, 67, 219, 149, 153, 203, 218, 328, 333, 204, 234, 227, 217, 128, 134, 287, 294	17.9to16	243, 67, 79, 271, 275, 260, 244, 272, 274, 68, 273, 78, 259, 245
-1.9to-0.1	150, 152, 254, 205, 216, 247, 274, 267, 151, 34, 28, 215, 206, 190, 191, 189, 329, 192, 332, 188, 193, 187, 194, 186, 195	15.9to14	69, 77, 246, 258, 70, 42, 43, 76, 41, 247, 71
0.0	214, 381, 207	13.9to12	44, 257, 75, 72, 60, 248, 74, 73, 45, 221, 222, 249, 256, 59, 240, 46, 223
0.1to1.9	196, 185, 108, 114, 197, 184, 54, 48, 198, 183, 308, 313, 199, 213, 182, 233, 228, 200, 181, 208,330, 331, 33, 29, 212, 209, 129, 133, 211, 210, 94, 88, 74, 68	11.9to10	250, 255, 239, 224, 58, 47, 251, 254, 252, 253, 225
2to3.9	32, 30, 253, 248, 288, 293 31, 232, 229, 273, 268, 130, 309, 132, 312	9.9to8	238, 48, 57, 226, 49, 237, 56, 50
4to5.9	53, 49, 231, 230, 131, 109, 113, 310, 311, 252	7.9to6	227, 55, 51, 236, 228, 54, 52, 53, 24, 23, 25, 22, 235, 229, 21
6to7.9	73, 69, 93, 89, 52, 289, 292, 50, 272, 269, 51, 110, 112, 251, 250	5.9to4	26, 40, 230, 234, 39, 27, 231, 233, 232, 38, 28, 37
8to9.9	290, 291, 111, 72, 70, 271, 270, 92, 90, 71	3.9to2	36, 205, 204, 29, 206, 203, 35, 207, 202, 201, 30, 208, 34, 220, 219, 217, 218, 216, 215, 31, 209, 33
10to11.9	91	1.9to0.1	32, 214, 210, 213, 212, 211, 181, 200, 182, 199, 190, 191, 189, 183, 192, 198, 188, 193, 184, 197, 187

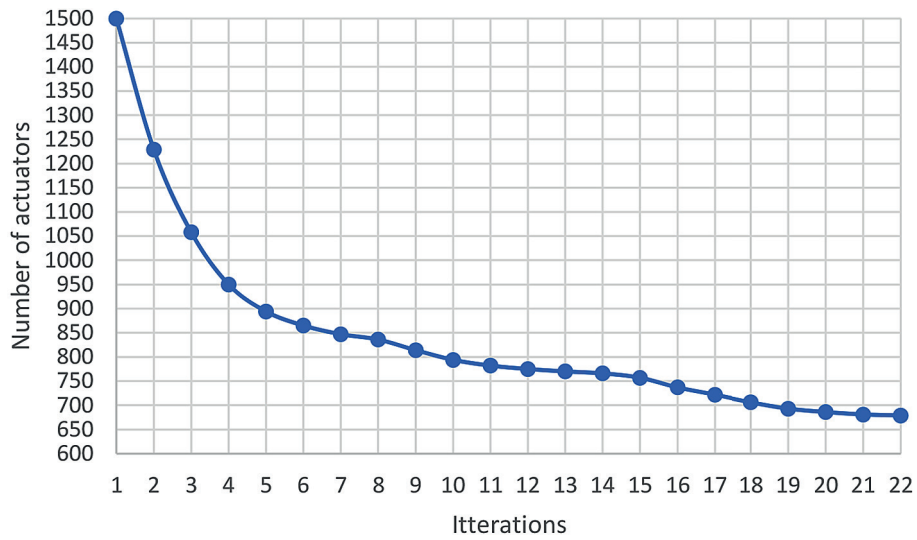


Figure 4. Optimality of the number of actuators in 22 steps

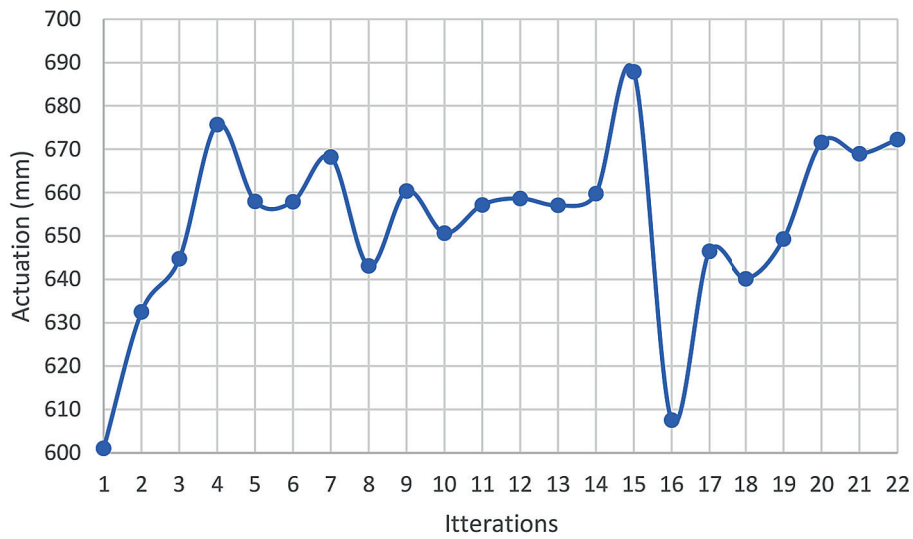


Figure 5. The amount of actuation in different trials

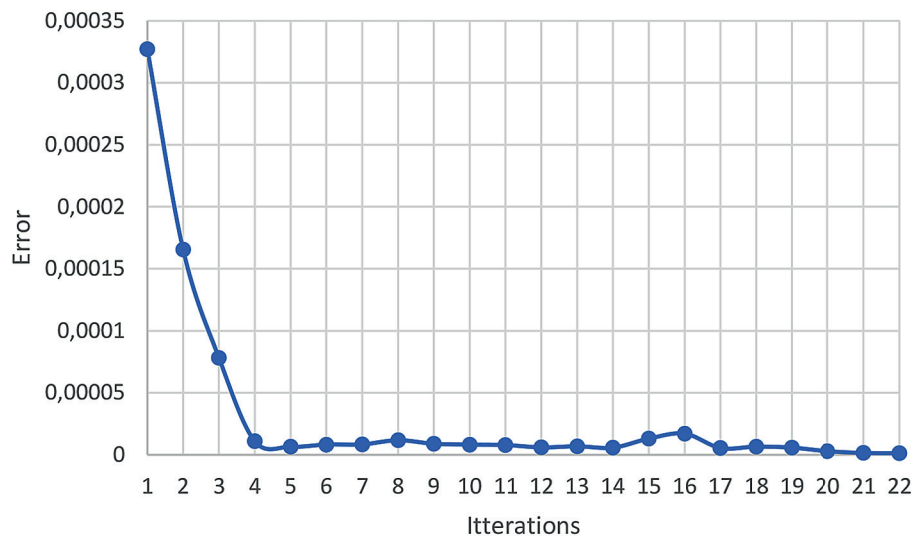


Figure 6. Error of the technique for obtaining the targets in different trials

Numerically speaking, 61% of the actuated members were lengthened while only 39% were shortened. The reason could be that the top joints were moved down, and the vertical members should be lengthened to take the joints to their original places. Whereas, the joints moved laterally through the effect of the horizontal loads were relocated

by shortening 39% of the actuated members. Table 2 shows that the large majority of the actuators were actuated in the range of $[0.1]$ to $[0.9]$. The table demonstrates that the percentage of the actuators that lengthened and shortened with the amount of 0.1 to 0.9 mm were 44 and

Table 2. The values of actuation of the actuators

Actuation (mm)	Actuator No.
-12.5	774
-11.99to-11	581
-9.99to-9	905
-7.9to-7	906
-3.9to-3	597, 1402, 859
-2.9to-2	855, 1401, 904, 253, 851, 226, 259, 202,
-1.9to-1	255, 246, 243, 260, 236, 242, 256, 228, 280, 275, 233, 277, 1453, 247, 268, 264, 258, 287, 274, 225, 606, 245, 279, 224, 262, 254, 272, 238, 209, 230, 249, 615, 298, 1454, 248, 270, 241, 296, 60, 216, 291, 244, 263, 317, 1430, 229, 896, 41, 619, 251, 223, 276, 1429, 284, 250, 1445, 221, 289, 234, 305, 257, 319, 300, 222, 293, 313, 231, 607, 232, 582, 266, 59, 47, 269, 44, 285, 1446, 45, 61, 999, 53, 46, 1284, 1283, 998, 283
-0.99to-0.9	288, 58, 297, 54, 55, 73, 42, 303, 316, 309, 52, 618, 43
-0.89to-0.8	574, 273, 62, 286, 314, 308, 57, 294, 64, 48, 307, 56, 281, 74, 265, 77, 892, 295
-0.79to-0.7	99, 339, 620, 1321, 1050, 50, 1397, 66, 271, 78, 63, 79, 51
-0.69to-0.6	567, 267, 301, 237, 282, 68, 278, 1480, 984, 103, 76, 1410, 67, 580, 72, 71, 82, 239, 261, 304, 85, 290, 563, 569, 81, 1457, 315, 985
-0.59to-0.5	1323, 292, 331, 240, 98, 1437, 575, 576, 562, 1409, 49, 227, 69, 65, 86, 871, 1399, 80, 561, 1018, 75, 573
-0.49to-0.4	116, 299, 751, 320, 578, 84, 572, 88, 564, 100, 1418, 70, 570, 1438, 565, 87, 302, 600, 602, 1097, 312, 329, 83
-0.39to-0.3	306, 102, 577, 29, 838, 211, 94, 771, 1350, 235, 1354, 104, 566, 252, 1220, 107, 101
-0.29to-0.2	1065, 571, 1199, 33, 28, 31, 1224, 1392, 32, 337, 26, 106, 1316, 568, 1466, 30, 97
-0.19to-0.1	35, 34, 125, 120, 318, 119, 1357, 27, 124, 752, 126
0.1to0.19	1302, 705, 1235, 376, 839, 1172, 154, 759, 1329, 1431, 687, 1333, 1253, 550, 362
0.2to0.29	1440, 1138, 1151, 645, 514, 158, 765, 149, 368, 1184, 369, 1117, 150, 542, 546, 1168, 366, 1249, 1008, 708, 201, 524, 661, 672, 1084, 1037
0.3to0.39	1017, 1093, 694, 684, 717, 142, 553, 157, 560, 677, 1306, 1211, 433, 156, 1188, 646, 1105, 152, 1142, 1089, 151, 775, 1088, 540, 159, 1177, 153, 197, 1264, 196, 675, 740, 686, 748, 670, 1338, 1075, 692, 328, 378, 1067
0.4to0.49	361, 166, 374, 169, 1046, 370, 515, 167, 1134, 750, 165, 1189, 192, 191, 1131, 141, 508, 363, 683, 189, 190, 168, 188, 651, 164, 1248, 155, 186, 551, 193, 1004, 178, 187, 380, 194, 179, 655, 648, 195, 177, 185, 1265, 739, 163, 180, 184, 1029, 1176, 170, 176, 1113, 679, 681, 917, 738
0.5to0.59	982, 364, 495, 162, 729, 543, 1146, 544, 654, 1062, 161, 175, 435, 160, 633, 492, 1112, 1058, 719, 171, 545, 1472, 693, 1054, 522, 172, 509, 518, 494, 173, 512
0.6to0.69	532, 426, 174, 1101, 1340, 857, 327, 897, 1471, 652, 644, 365, 695, 432, 517, 520, 506, 678, 643, 967, 436, 523, 552, 723, 995, 747, 753, 428, 423, 559, 660, 611, 408
0.7to0.79	1009, 656, 504, 533, 510, 877, 521, 475, 924, 425, 945, 471, 632, 1036, 881, 746, 491, 488, 953, 497, 434, 421
0.8to0.89	440, 503, 473, 691, 902, 516, 990, 424, 490, 507, 690, 429, 853, 511, 483, 531, 431, 467, 427, 925, 484, 476, 1025, 755, 628, 1021, 539
0.9to0.99	612, 609, 1013, 757, 463, 469, 728, 367, 525, 466, 727, 756, 455, 453, 974, 642, 971, 486, 496, 446, 443, 778, 777, 457, 481, 696, 861, 411, 381, 382, 383, 384, 385, 386, 387, 388, 389, 390, 391, 392, 393, 394, 395, 396, 397, 398, 399, 400, 415, 438
1to1.9	485, 464, 634, 459, 430, 487, 456, 658, 502, 929, 478, 450, 452, 1100, 493, 889, 505, 448, 472, 501, 760, 499, 489, 933, 449, 444, 198, 498, 414, 631, 714, 513, 734, 447, 627, 451, 482, 613, 763, 442, 948, 470, 519, 407, 461, 468, 477, 409, 978, 458, 736, 445, 937, 465, 841, 659, 500, 641, 460, 749, 454, 781, 949, 480, 1051, 441, 770, 474, 630, 766, 479, 941, 772, 462, 865, 638, 418, 894, 417, 657, 886, 845, 416, 402, 403, 405, 711, 890
2to2.9	869, 404, 406, 625, 419, 873, 401, 624, 868, 420, 635, 622, 623, 626, 910, 768, 621, 899, 639, 636
3to3.9	761, 864, 805, 806
4to4.9	640
7to7.9	601
10to10.9	637
18.45	794

24 respectively. Furthermore, only 6% of the actuators were actuated with values greater than 1.9|mm.

Table 3 tabulated the members with internal force above 30kN either in tension or compression before and after adjustment. It can be seen that none of the members exceed the elastic range before and after adjustment. Furthermore, the number of members whose internal force was above 70kN was only 3, which tripled after actuating the actuators. Nonetheless, some members were in tension before adjustment, while their phases changed to compression after adjustment. The changes occurred because some of these members were lengthened; for example, the internal force Member 198 before adjustment was 1788, the member was lengthened by 1.17mm as presented in Table 2, and its internal force became -74218 after actuation. The members with significant changes in their internal force were tabulated in Table 4. Some other members were already in compression before adjustment; after actuation, their compression value increased. For example, Member 174, which was lengthened by 0.45, its

internal force before and after adjustment was -10900N and -56590N, respectively.

Table 4 shows the members with the significant change in their internal force after adjustment. The internal force of the members in (Column (1), Table 4) was changed by up to 76372N. Furthermore, some members changed their phase and some others reduced their tension or compression state, the changes were illustrated in Figure 7. The figure shows that the number of members whose compression force increased was 428; on the other hand, the tension state increased in 280 members. Furthermore, 248 members changed their phase from compression to tension, whereas 79 members changed from tension to compression. Moreover, the number of members that reduced their compression and tension force were 242 and 126, respectively.

Another attempt has been made, by changing the minimum limit of actuation per actuator from 0.1 mm to 0.15mm to see the possibility of reduction of the actuator numbers. Figure 8 shows the number of active actuators in four trials while the minimum limit of actuation per

Table 3. The member with the internal force in the range of 30to74.2kN either in tension or in compression before and after adjustment using MATLAB and SAP2000

Status	Force (kN)	Members before adjustment	Members after adjustment
Compression	-74.2 to -70	857, 853, 861	182, 183,185, 186, 187, 188, 189, 190, 191, 192, 193, 194, 195, 196, 197, 198, 200, 640, 857, 861, 865, 902, 910, 184, 853, 199, 181, 621, 894
	-69.9 to -60	849, 640, 401, 621, 420, 639, 402, 865, 622, 638, 419, 623, 403	845, 639, 622, 637, 869, 841, 886, 420, 636, 906, 401, 419, 638
	-59.9 to -50	845, 637, 624, 418, 902, 404, 906, 869, 636, 625, 898, 910	624, 365, 406, 404, 366, 364, 367, 174, 625, 405, 403, 633, 363, 402, 173, 416, 172, 623, 627, 626, 417, 171, 873, 362, 418, 368, 635
	-49.9 to -40	417, 626, 405,635, 841, 894, 660, 641, 627, 659, 634, 642, 658, 914, 643, 406, 416, 628, 873	175, 161, 361, 462, 890, 162, 657, 632 917, 849, 479, 659, 369, 176, 642, 170, 641, 380, 180, 163, 474, 630, 658, 634, 177, 441, 628, 179, 178, 480
	-39.9 to -30	657, 633, 644, 629, 656, 632, 645, 630,890, 631, 917, 407, 646, 655,415, 647, 920, 654	164, 168, 454, 460, 631, 500, 370, 379, 165, 465, 167, 877, 445, 169, 643, 166, 458, 409, 477, 644, 468, 461, 407, 519,470, 442, 656, 482, 378, 451, 646, 655, 913, 864, 447, 513, 881, 414, 498, 444, 449, 660, 489, 499, 501, 472, 448, 505, 645, 493, 648, 766, 941, 452, 371
Tension	39.9 to 30	30, 31, 232, 229, 863, 29, 257, 851, 56, 243, 45, 231, 32, 230, 28, 256, 46, 244, 55, 33, 47, 27, 54, 245, 255, 34, 867, 48, 847, 53, 49, 246, 254, 904, 52, 908, 50, 26, 51, 35, 80, 61, 79	245, 912, 246, 59, 233, 893, 900, 47, 254, 44, 847, 244, 45, 53, 46, 249, 904, 58, 874, 908, 214, 54, 55, 42, 275, 896, 871, 277, 247, 870, 52, 866, 274, 207, 43, 57, 61, 862, 262, 48, 268, 56, 360
	49.9 to 40	236, 224, 225, 235, 226, 234, 60, 41, 59, 42, 58, 260, 227, 859, 259, 855, 43, 233, 241, 258, 57, 228, 44, 242	239, 867, 235, 259, 240, 242, 256, 258, 60, 228, 255, 232, 859, 41, 863, 226, 227, 851, 855, 229, 243, 260, 234, 241, 257
	59.9 to 50	240, 239, 221, 238, 222, 237, 223	224, 225, 222, 223, 230, 231, 237
	69.9 to 60		238, 221, 236

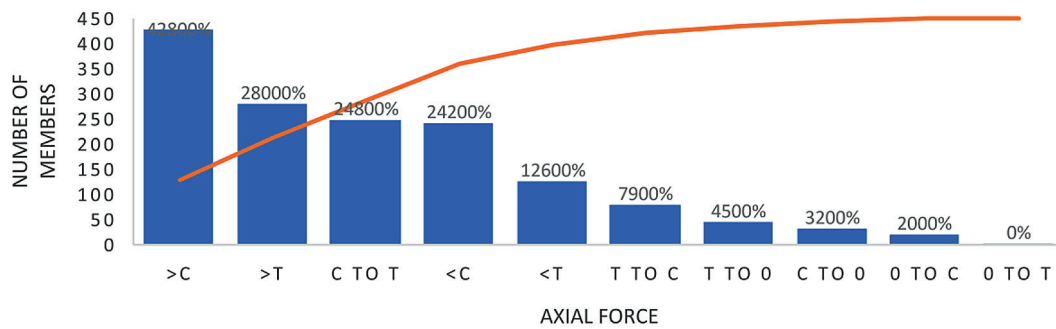


Figure 7. Phase changing of the members after adjustment

actuator is 0.15 mm. It can be seen from the figure that; the optimum number of actuators was 809. In comparison, it was 679 when the minimum limit was 0.1 mm.

Other attempts have been made with different limits as the minimum amount of actuation per actuator. Figure 9 illustrates that, by decreasing the limit, the number of active members were declined. Furthermore, the optimum number of actuators was attained when the limit was 0.1 mm. Though the number of actuators may fall by decreasing the limit, actuation with less than 0.1 mm may not be applicable. For this reason, 0.1 mm has been chosen as the minimum limit, and the minimum number of actuators was 679 mm.

CONCLUSIONS

A numerical model of a double-layer spherical pin-jointed structure was loaded vertically and laterally simultaneously, which caused a significant deformation. The displaced exterior layer joints were relocated to their original positions; meanwhile, the stress in all members was kept within the elastic range. The targets were obtained with the minimum possible number of actuators (679) with total actuation of 672 mm after 22 iterations. Furthermore, it was found that the number of actuators declines by reducing the limit of actuation. The optimum number of actuators was obtained

Table 4. The members with significant changes of stress after adjustment

1				2				3			
Memr	tp(N)	ta(N)	ta-tp	Mem	tp(N)	ta(N)	ta-tp	Mem	tp(N)	ta(N)	ta-tp
200	2154	-74218	-76372	173	-11245	-54611	-43366	849	-67590	-45479	22111
199	2055	-73978	-76033	172	-11312	-54020	-42708	347	-6865	15712	22577
182	1813	-74218	-76031	886	-22913	-64148	-41235	350	-8084	14501	22585
198	1788	-74218	-76006	171	-11017	-51503	-40486	351	-8349	15203	23552
181	2072	-73594	-75666	365	-19428	-59450	-40022	569	-6699	17438	24137
183	1401	-74218	-75619	161	-9842	-49332	-39490	580	-5974	18256	24230
197	1377	-74218	-75595	175	-10382	-49447	-39065	342	-6837	17817	24654
196	862	-74218	-75080	366	-19219	-58058	-38839	567	-6083	19767	25850
184	877	-74203	-75080	364	-19636	-57964	-38328	218	-2859	23488	26347
185	293	-74218	-74511	367	-19068	-57194	-38126	354	-7481	19008	26489
195	293	-74218	-74511	162	-10357	-46973	-36616	893	10833	37571	26738
194	-275	-74218	-73943	363	-19787	-54945	-35158	353	-7968	18791	26759
186	-290	-74218	-73928	176	-9806	-44077	-34271	355	-6903	20032	26935
193	-790	-74218	-73428	180	-9172	-43036	-33865	352	-8281	19372	27653
187	-814	-74218	-73404	170	-10346	-43794	-33448	898	-52552	-24502	28050
192	-1201	-74218	-73017	179	-8876	-41339	-32463	359	-5456	23610	29066
188	-1226	-74218	-72992	177	-9289	-41678	-32389	574	-4795	25292	30087
191	-1468	-74218	-72750	163	-10557	-42901	-32344	885	-2464	28012	30476
189	-1485	-74218	-72733	178	-8944	-40577	-31633	341	-6524	24068	30592
190	-1567	-74218	-72651	368	-19039	-50613	-31574	909	-9077	21705	30782
174	-10900	-56590	-45690	362	-19816	-50888	-31072	360	-5722	30106	35828

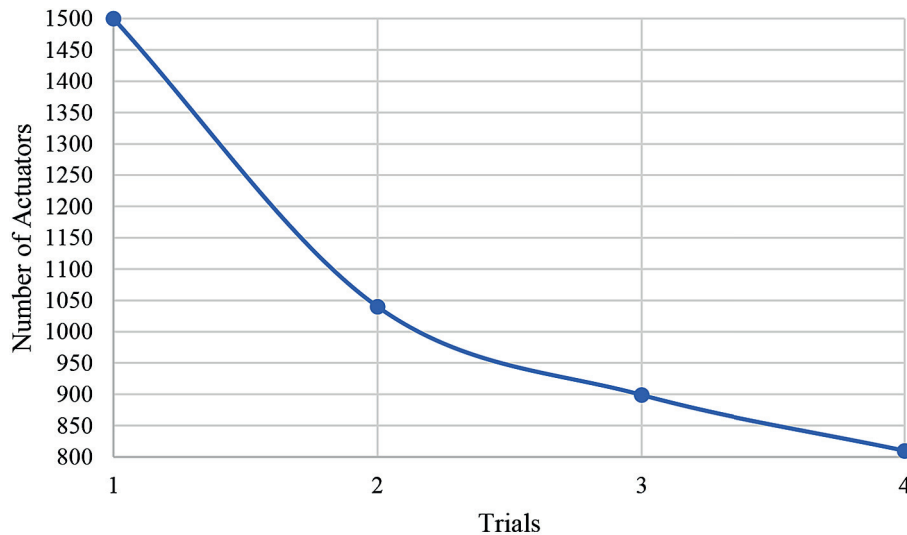


Figure 8. Minimization of used actuators in 4 trials when the minimum limit of actuation is 0.15 mm

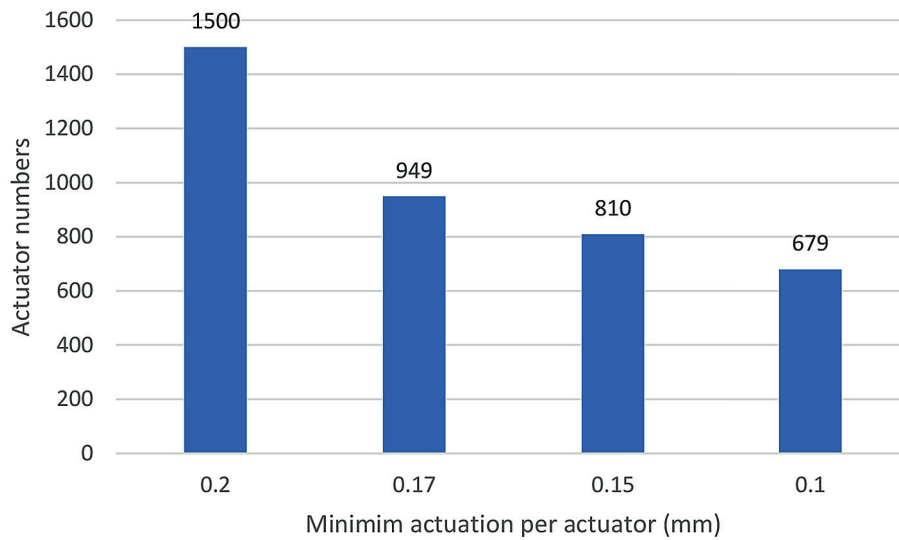


Figure 9. Optimum number of actuators with different limits of actuation per actuator

when the limit of actuation per actuator was 0.1 mm. It should be noted that the significant change in the internal force of some members was determined, but none of the members exceeded the limit. Another finding in the research was; almost two-thirds of the actuators were lengthened, while the rest were shortened. This was because a substantial effort was needed to bring up the joints that were moved downward. Most active actuators were actuated within the range of 0.1 to 0.9 mm. In addition, the dissimilarity between the obtained results and the targets was almost null. Finally, the results obtained in the MATLAB program were verified by SAP2000 software.

REFERENCES

1. Bechmann, R., et al., Eine runde Sache: Stahl-Glas-Tragwerke für die EXPO 2017 in Astana. *Stahlbau*, 2019; 88(1). 57-63. <https://doi.org/10.1002/stab.201800022>
2. Winterstetter, T., et al., Innovative Bautechnik im Herzen Asiens–die EXPO 2017 in Astana, Kasachstan. *ce/papers*, 2018; 2(1). 51-57. <https://doi.org/10.1002/cepa.630>
3. Chang, X. and Haiyan, X. Using sphere parameters to detect construction quality of spherical buildings. in 2010 2nd International Conference on Advanced Computer Control. <https://doi.org/10.1109/ICACC.2010.5487073>
4. Irschik, H., A review on static and dynamic shape control of structures by piezoelectric actuation.

- Engineering Structures, 2002; 24(1). 5-11. [http://dx.doi.org/10.1016/S0141-0296\(01\)00081-5](http://dx.doi.org/10.1016/S0141-0296(01)00081-5)
5. Haftka, R.T., Limits on static shape control for space structures. *AIAA Journal*, 1991; 29(11). 1945-1950. <https://doi.org/10.2514/3.10823>
 6. Hu, Y.-R. and Vukovich, G., Active robust shape control of flexible structures. *Mechatronics*, 2005; 15(7). 807-820. <https://doi.org/10.1016/j.mechatronics.2005.02.004>
 7. Koconis, D.B., Kollar, L.P., Springer, G.S., Shape control of composite plates and shells with embedded actuators. II. Desired shape specified. *Journal of Composite Materials*, 1994; 28(3). 262-285.
 8. Hadjigeorgiou, E., Stavroulakis, G., and Massalas, C., Shape control and damage identification of beams using piezoelectric actuation and genetic optimization. *International Journal of Engineering Science*, 2006; 44(7). 409-421. <https://doi.org/10.1016/j.ijengsci.2006.02.004>
 9. Haftka, R.T., Adelman, H.M., Effect of sensor and actuator errors on static shape control for large space structures. *AIAA Journal*, 1987; 25(1). 134-138. <https://doi.org/10.2514/3.9592>
 10. Salama, M., et al., Shape adjustment of precision truss structures: analytical and experimental validation. *Smart Materials and Structures*, 1993; 2(4). 240. <https://doi.org/10.1088/0964-1726/2/4/005>
 11. Saeed, N.M., Kwan, A.S.K., Simultaneous displacement and internal force prescription in shape control of pin-jointed assemblies. *AIAA journal*, 2016; 54(8). 2499-2506. <https://doi.org/10.2514/1.J054811>
 12. Weeks, C.J., Static shape determination and control of large space structures: I. The flexible beam. *Journal of Dynamic Systems, Measurement, and Control*, 1984; 106(4). 261-266. <http://dx.doi.org/10.1115/1.3140683>
 13. Haftka, R.T., Adelman, H.M., An analytical investigation of shape control of large space structures by applied temperatures. *AIAA Journal*, 1985; 23(3). 450-457. <http://dx.doi.org/10.2514/3.8934>
 14. Ziegler, F., Computational aspects of structural shape control. *Computers & Structures*, 2005; 83(15). 1191-1204. <http://dx.doi.org/10.1016/j.compstruc.2004.08.026>
 15. Yuan, S., Yang, B. Shape adjustment of large deployable mesh reflectors under thermal strain. in *AIAA Scitech 2021 Forum*, 2021 1148. <https://doi.org/10.2514/6.2021-1148>
 16. Yuan, S., Yang, B., Fang, H. Improvement of surface accuracy for large deployable mesh reflectors. in *AIAA/AAS Astrodynamics Specialist Conference*. 2016 5571. <https://doi.org/10.2514/6.2016-5571>
 17. Christoforou, E.G., et al., Design and control concept for reconfigurable architecture. *Journal of Mechanical Design*, 2015; 137(4). 042302. <https://doi.org/10.1115/1.4029617>
 18. You, Z., Displacement control of prestressed structures. *Computer Methods in Applied Mechanics and Engineering*, 1997; 144(1). 51-59. [http://dx.doi.org/10.1016/S0045-7825\(96\)01164-4](http://dx.doi.org/10.1016/S0045-7825(96)01164-4)
 19. Wang, Z., Li, T., Cao, Y., Active shape adjustment of cable net structures with PZT actuators. *Aerospace Science and Technology*, 2013; 26(1). 160-168. <https://doi.org/10.1016/j.ast.2012.03.001>
 20. Manguri, A.A., Kwan, A.S.K., Saeed, N.M., Adjustment for shape restoration and force control of cable arch stayed bridges. *International Journal of Computational Methods and Experimental Measurements*, 2017; 5(4). 514-521. <http://dx.doi.org/10.2495/CMEM-V5-N4-514-521>
 21. Du, J., Zong, Y., Bao, H., Shape adjustment of cable mesh antennas using sequential quadratic programming. *Aerospace Science and Technology*, 2013; 30(1). 26-32. <http://dx.doi.org/10.1016/j.ast.2013.06.002>
 22. Kabando, E.K., Gong, J., An overview of long-span spatial grid structures failure case studies. *Asian Journal of Civil Engineering*, 2019; 20(8). 1137-1152. <https://doi.org/10.1007/s42107-019-00168-4>
 23. Kwan, A.S.K., Pellegrino, S., Prestressing a space structure. *AIAA Journal*, 1993; 31(10). 1961-1963. <http://dx.doi.org/10.2514/3.11876>
 24. Kawaguchi, K.-I., et al., Shape and stress control analysis of prestressed truss structures. *Journal of Reinforced Plastics Composites*, 1996; 15(12). 1226-1236. <https://doi.org/10.1177/073168449601501204>
 25. Irschik, H., Ziegler, F., Eigenstrain without stress and static shape control of structures. *AIAA journal*, 2001; 39(10). 1985-1990. <https://doi.org/10.2514/2.1189>
 26. Shen, L.Y., Li, G.Q., Luo, Y.F., Displacement control of prestressed cable structures (in Chinese). *Journal of Tongji University(Natural Science)*, 2006; 34(3). 291-295. http://en.cnki.com.cn/article_en/cjfdtotal-tjdz200603001.htm
 27. Xu, X., Luo, Y.Z., Non-linear displacement control of prestressed cable structures. *Proceedings of the Institution of Mechanical Engineers, Part G: Journal of Aerospace Engineering*, 2009; 223(7). 1001-1007. <https://doi.org/10.1243/09544100JAERO455>
 28. Kaveh, A., *Optimal structural analysis*. John Wiley & Sons, 2014.
 29. Sabadka, D., Molnar, V., Fedorko, G., The use of lean manufacturing techniques–SMED analysis to optimization of the production process. *Advances in Science Technology. Research Journal*, 2017; 11(3). <http://dx.doi.org/10.12913/22998624/76067>

30. Furuya, H., Haftka, R.T., Placing actuators on space structures by genetic algorithms and effectiveness indices. *Structural Optimization*, 1995; 9(2). 69-75. <https://doi.org/10.1007/BF01758822>
31. Yuan, S., Jing, W., Optimal Shape Adjustment of Large High-Precision Cable Network Structures. *AIAA Journal*, 2021; 59(4). 1441-1456. <https://doi.org/10.2514/1.J059989>
32. Saeed, N.M., Manguri, A.A.H., Adabar, A.M., Shape and force control of cable structures with minimal actuators and actuation. *International Journal of Space Structures*, 2021; 36(3). 241-248. <https://doi.org/10.1177/09560599211045851>
33. Mahmood, A., et al. Optimized Stress and Geometry Control of Spherical structures under Lateral Loadings. in 2022 8th International Engineering Conference on Sustainable Technology and Development (IEC). 2022; 142-148. <http://dx.doi.org/10.1109/IEC54822.2022.9807455>
34. Manguri, A., Saeed, N., Haydar, B. Optimal Shape Refurbishment of Distorted Dome Structure with Safeguarding of Member Stress. in 7th International Engineering Conference “Research & Innovation amid Global Pandemic”(IEC). Erbil, Iraq, 2021; 90-95. <https://doi.org/10.1109/IEC52205.2021.9476107>
35. Saeed, N., Manguri, A., Al-Zahawi, S. Optimum Geometry and Stress Control of Deformed Double Layer Dome for Gravity and Lateral Loads. in 2021 7th International Engineering Conference “Research & Innovation amid Global Pandemic”(IEC). Erbil, Iraq, 2021, 84-89. <https://doi.org/10.1109/IEC52205.2021.9476094>
36. Nocedal, J., Wright, S., Numerical optimization. Second Edition ed., New York: Springer Science & Business Media; 2006.
37. Chen, W.F., Lui, E.M., Handbook of structural engineering. CRC press, 2005.